An Unmanned Aircraft System for Automatic Forest Fire Monitoring and Measurement

Luis Merino · Fernando Caballero
J.R. Martínez-de-Dios · Iván Maza
Aníbal Ollero

Abstract The paper presents an Unmanned Aircraft System (UAS) for forest fire monitoring, consisting of several aerial vehicles and a central station. Fire monitoring is defined as the computation in real-time of the evolution of the fire front shape and potentially other parameters related to the fire propagation, and is very important for forest fire fighting. The paper shows how an UAS can automatically obtain this information by means of on-board infrared or visual cameras. Moreover, it is shown how multiple aerial vehicles can collaborate in this application, allowing to cover bigger areas or to obtain complementary views of a fire. The paper presents results obtained in experiments considering actual controlled forest fires in quasi-operational conditions, involving a fleet of three vehicles, two autonomous helicopters and one blimp.

Keywords forest fire fighting · UAS · cooperative perception

1 Introduction

Hundreds of thousands of hectares are devastated by wildfires each year. Forest fires lead to the destruction of forest and the wildlife that inhabits them, and have a disastrous social, economic and environmental impact. Forest fire fighting involves extensive

————————————————
L. Merino
Pablo de Olavide University, Crta. Utrera, km.1, 41013, Seville (Spain)
E-mail: lmercab@upo.es

F. Caballero, J.R. Martínez-de-Dios, I. Maza and A. Ollero
Universidad de Sevilla, Escuela Superior de Ingenieros, Camino de los Descubrimientos s/n, 41092 Sevilla (Spain)
Tel.: +34-954-487361
Fax: +34-954-487340
E-mail: imaza@us.es, fcaballero@us.es, jdedios@cartuja.us.es, aollero@cartuja.us.es

A. Ollero
Center for Advanced Aerospace Technology (CATEC), Parque Tecnológico y Aeronáutico de Andalucía, C. Wilbur y Orville Wright 17-19-21, 41309, La Rinconada (Spain)
E-mail: aollero@catec.aero

Fig. 1 Different stages in the evolution of a fire.

human resources, and is a very dangerous activity, which originates many casualties every year. In many cases, the lack of information about the dynamic evolution of fire plays an important role in these accidents. Figure 1 shows the state of a experimental controlled fire at several time instants. Among the most important parameters for fire fighting management are: the shape and position of the fire front, its rate of spread (how this front evolves with time) and the maximum height of the flames [37]. If available, this information, integrated within a Geographical Information System (GIS), can be used by the fire brigades for fire fighting planning, for instance by predicting the potential evolution of the fire, determining the optimal location of fighting means, etc. Fire monitoring can be defined as the estimation in real-time of the evolution of these parameters.

Forest-fire fighting is commonly based on estimations made by fire fighting experts from visual observations. These estimations are subject to a great number of errors due to smoke occluding the flames, human inaccuracy in the visual estimation and errors in the localization of the fire. Recently, new technologies have been applied to fire fighting. However, many of these technologies still have different practical problems for their use in operational conditions, such as low reliability, high costs and others.

Unmanned Aircraft Systems (UAS) can play an important role for forest fire response. They have been already successfully demonstrated for fire detection, localization and observation (as in [2, 28, 26, 25]). In this paper, an UAS for automatic real-time forest fire monitoring and measurement is presented. The extension of a forest fire can be very large, so the system can integrate information from several aerial vehicles, that can collaborate to cover the fire from complementary points of view. The system is able to provide, in real-time, of the current position of the fire front in geographical coordinates.

The paper begins with a description of some current automatic approaches for forest fire fighting that can be found in the literature. Then, it presents the UAS for fire monitoring, the vehicles and modules involved; then, it focuses on the data fusion and image processing techniques employed. Results from experiments involving controlled forest fires are described at the end of the paper, before the conclusions.

1.1 Related work

Traditionally, information extraction for fire fighting support has been done by experts, directly on the terrain or analyzing data provided by towers, satellites or other means. However, some systems have been developed in order to automatically extract the relevant information from several sources of information.

Most automatic systems for fire detection are based on cameras placed on ground as, for example, the BOSQUE system, which relies on infrared cameras and automatic image processing techniques for fire detection, including false alarm rejection [3]. Colour ground cameras are also used for autonomous detection of forest fires [7,9]. Some systems are based on smoke plume detection algorithms [8,12]. Other sensors have been also employed for automatic forest fire detection, like LIDAR [36], due to its interesting characteristics for smoke plume detection in situations where visual cameras cannot operate (as, for instance, during night). These systems have some drawbacks, such as the coverage and the lack of reliability of the automatic detection in changing environmental conditions.

The use of satellites for fire detection has been also considered [35,18]. Besides, manned airborne-based systems have been also used, like in the Airborne Wildfire Intelligence System (AWIS), in Canada [4]. The use of Unmanned Aerial Vehicles (UAVs) for automatic forest fire detection has been considered by the authors [28]. Also, the design of a infrared vision system for UAS in fire missions is considered in [19].

Fire monitoring is usually performed by experts, that estimate, visually or from images gathered by cameras, the rate of spread and height of the flames. More recently, airborne systems are used in order to have a broad overview of the fire evolution, but still the monitoring activities are carried out by people. Satellite-based systems have been also proposed for forest fire monitoring [6,13,35]. The temporal and spatial resolutions of these systems are still very low for the requirements of forest-fire fighting in many cases. There are some fire analysis techniques based on computer vision for fires carried out in laboratories, as [22,32]. However, the application of the same techniques to non-controlled outdoor environments is not considered in those papers.

This paper presents the application of aerial robots for the fire monitoring. As mentioned, manned helicopters or airplanes are often used, but they are expensive and there is a high risk for humans involved in the operation. The use of UAVs can help to reduce the risk associated to manned aircrafts close to fire.

The use of UAVs in forest-fire fighting scenarios has been analyzed in the FiRE project in the United States. The ALTUS UAV, an evolution of the Predator UAV, has been demonstrated in fire experiments in the FiRE project [1]. The data received at the ground station are geo-referenced imagery about the fire, sent through satellite uplink/downlink channels.

While the FiRE project considers a single and complex UAV with complex sensors on these tasks, the COMETS European project addressed the use of a team of sim-
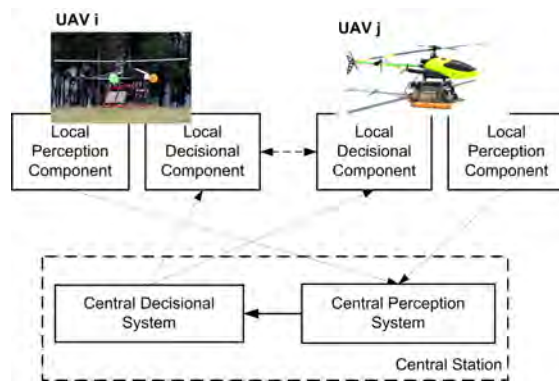
Fig. 2 The system consists of several vehicles and two main components: the decisional system and the perception system.

pler UAVs that cooperate in fire detection and monitoring tasks [31]. Very few work has been identified considering multiple UAVs in the task of fire perception. One of them is the work presented in [5], where the feasibility of the application of a team of small (low-altitude, short endurance) aerial systems to cooperatively monitor and track the propagation of large forest fires is explored. The paper deals with path planning activities, and provides simulations using a six degree of freedom dynamic model for the vehicles and a numerical propagation model for the forest fire. However, results in actual fire fighting activities are still to come. Also, in [42], the authors present a method for orthorectification of images gathered from an UAV, for their application in fire monitoring activities. They discuss specific problems that have to be solved in the case of forest areas, and present very preliminary results on aerial images gathered from a conventional aircraft. However, no actual fire monitoring results are presented.

2 An Unmanned Aircraft System for fire monitoring

The UAS described in this paper is composed of a team of aerial vehicles and a central station. This section summarizes the requirements and principal software modules at the level of the whole system (see Figure 2).

2.1 Vehicles and Sensors

The system developed is able to coordinate heterogeneous unmanned vehicles for fire monitoring. The only requirements on these UAVs are the following:

Operational autonomy: the UAVs should be able to fly waypoints and to hover (or pseudo-hover in the case of planes) at given places autonomously.
Localization: they should be able to localize themselves on the same reference frame.
Perception payload: they should carry infrared and/or visual cameras for perception purposes.

The system has been tested with a fleet of two helicopters and one blimp. In this case, the vehicles are equipped with differential GPS receivers and Inertial Mea-

Fig. 3 The vehicles carry mainly IMUs and GPS for navigation. Also, cameras on pan and tilt units for perception.

surement Units (IMUs) which allow them to localize themselves in a common world reference frame.

Besides, for perception purposes the vehicles carry infrared and visual cameras and, some of them, pan and tilt units. Figure 3 shows some examples. As it can be seen, one of the UAVs carry a low-cost non-thermal OEM infrared micro-camera in the far infrared band (7-14 microns), besides a visual camera. All the cameras in the system are calibrated before the flights by using artificial patterns. All the images gathered are tagged locally with the composed pose and orientation of the vehicle and the pan and tilt unit, timestamps and calibration information.

Moreover, the UAVs carry on board communication devices to be able to receive commands from the ground station, and to send information back to it.

2.2 Decision-making system

The difference between UAS and manned systems is their ability to perform autonomously certain tasks. As commented above, the system presented here only requires that the vehicles are able to autonomously navigate between waypoints. However, the fire monitoring missions are high-level tasks that require a decisional system for the coordination and control of the fleet of aerial autonomous vehicles of the system. This decisional system implements four main different mechanisms:

Task Allocation arises in a multi-Unmanned Aerial System, where each of the UAS is able to perform tasks in response to the tasks requests. The issue is to decide which system should be endowed with each given task to be performed (for instance, which UAS should go to the different viewpoints to observe the fire). This requires the capability to assess the interest of assigning a certain system to a given task. This operation is especially difficult when the decision has to be done taking into account the current individual plans of the UAS as well as the tasks left to be assigned [39, 21, 40].

Task Planning is a central issue of the decisional components. It aims at building a sequence of basic tasks to perform, in order to achieve a given high level mission, for instance a fire monitoring mission.

Coordination is a process that arises within a system if given resources (either internal or external) are simultaneously required by several components of this system. In the case of a multi-UAV system, a classic coordination issue to deal with is the sharing of space between the different vehicles, to ensure that each vehicle will be able to perform its plan safely and coherently regarding the plans of the other systems. For instance, as a fire detection mission involves complete coverage of a given area, the region should be divided among the available systems

Algorithm 1 $\{f_{k,t}, q_{k,t}\} \leftarrow \text{Filter}(\{f_{k,t-1}, q_{k,t-1}\}, \mathbf{z}_t)$

1: **for all** k **do**

2: $\quad \bar{f}_{k,t} = (1 - q_{k,t-1})(f_{k,t-1} + \frac{1}{|R(k)|} \sum_{j \in R(k)} \omega_j f_{j,t-1})$

3: $\quad \bar{q}_{k,t} = q_{k,t-1} + (1 - q_{k,t-1})(\beta \bar{f}_{k,t-1})$

4: $\quad f_{k,t} = \frac{\bar{f}_{k,t} p(\mathbf{z}_t | F_{k,t}=1)}{\bar{f}_{k,t} p(\mathbf{z}_t | F_{k,t}=1) + (1-\bar{f}_{k,t}) p(\mathbf{z}_t | F_{k,t}=0)}$

5: $\quad q_{k,t} = \frac{\bar{q}_{k,t} p(\mathbf{z}_t | Q_{k,t}=1)}{\bar{q}_{k,t} p(\mathbf{z}_t | Q_{k,t}=1) + (1-\bar{q}_{k,t}) p(\mathbf{z}_t | Q_{k,t}=0)}$

6: **end for**

accordingly with their relative capabilities (such as maximum speed, autonomy, field of view of the cameras, etc.).

Another example can be found in the context of fire monitoring: several synchronized perceptions of the event are required with convenient locations and orientations of the involved cameras.

Supervision deals with the management (control) of the tasks execution, in several ways:

- A first concern is simply to keep the system aware of the tasks processing evolution during their executions ;
- A second concern is to detect the possible tasks failures and (if possible) to react to such events in a way that will prevent the system to fail.

The decisional system employed in our UAS is described in detail in [11,20], and is able to cope with the previous issues. In Section 6 an example of the capabilities of this system will be shown.

3 Perception system description

The system considers all the information gathered by the different UAVs in our system to estimate the evolution of the fire applying data fusion techniques. The general picture is given by Fig. 4. In the system, each vehicle will locally process its images and provide features related to the fire front evolution. All this information is received at the central station, in which the estimation takes place, taking into account all the data from the fleet.

The first issue is to devise a convenient representation of the information related to the fire. The fire is a dynamic object that propagates, changing in size and shape. The representation chosen here for autonomous perception consists of an evidence grid. The area is divided into a rectangular grid, in which the state of each cell k is defined by two binary values: $F_{k,t} \in \{0,1\}$, indicating if there is fire in the cell, and $Q_{k,t} \in \{0,1\}$, indicating if the fuel in the cell is completely exhausted.

The system cannot be certain about these values, and therefore, two probability values $\{f_k, q_k\}$ are stored for each cell. These two values correspond to the probabilities $f_k = p(F_{k,t} = 1)$ (there is fire at a given cell), and $q_k = p(Q_{k,t} = 1)$ (the fuel in that cell is completely exhausted). Each cell also has an associated 3-D position $\mathbf{p}_k$, given by a digital elevation map that is previously loaded in the system (and that can be the result of a previous mapping mission [16]). The system should obtain online an estimation of these values for all the cells of the grid by using all the data gathered by the system up to time t, $\mathbf{z}^t$.
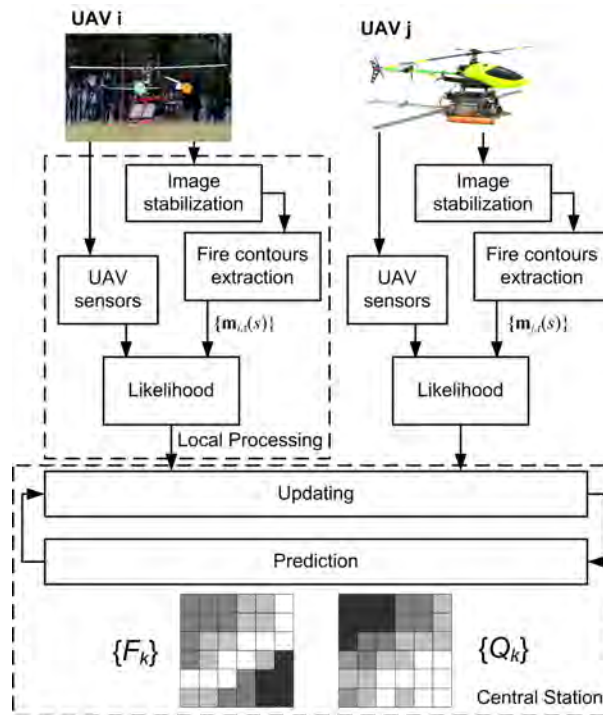
Fig. 4 The system estimates two probability grids (fire presence and fuel at each cell). The state of the grids is estimated incorporating data obtained from the fleet of UAVs. The prediction step incorporates the increase in uncertainty due to the motion of the fire.

The integration of new information provided by the UAS is done by using a discrete Bayes Filter for each cell of the grid, summarized in Alg. 1. The steps involved in the estimation are summarized in Fig. 4. Next sections will describe the different blocks depicted in the figure.

3.1 Prediction model

As shown in Fig. 4, the system allows considering a prediction step in the estimation, so that fire propagation models could be included. There are many aspects that influence the propagation of fire, like the slope of the terrain, the moisture content of the vegetation, the meteorological conditions -wind, air humidity, etc- [37]. It is not the objective of this paper to deal with these aspects. The prediction model depicted here is very simple, and considers two different relations: a temporal relation and a spatial relation among cells. Its main objective is, in one hand, to incorporate a kind of memory in the estimation process, so that the fire does not propagate "backwards" through zones previously visited (this is the role of Q). Also, a spatial prediction is performed in order to smooth the estimated evolution of the fire fronts.

Although there is a separated filter for each variable, both are not independent, and therefore the dependence should be marginalized out during the prediction phase. The temporal transition probability for each cell can be decomposed as:

$$p(F_{k,t}|F_{k,t-1}) = \sum_{Q_{k,t-1}} p(F_{k,t}|F_{k,t-1},Q_{k,t-1})p(Q_{k,t-1}) \tag{1}$$

$$p(Q_{k,t}|Q_{k,t-1}) = \sum_{F_{k,t-1}} p(Q_{k,t}|F_{k,t-1},Q_{k,t-1})p(F_{k,t-1}) \tag{2}$$

The different terms are characterized by one main parameter, β, which is the probability that a cell is completely exhausted if there was fire the previous time instant:

$$p(Q_{k,t}=1|F_{k,t-1},Q_{k,t-1}) = \begin{cases} 1 & \text{if } Q_{k,t-1}=1 \\ 0 & \text{if } Q_{k,t-1}=0 \text{ and } F_{k,t-1}=0 \\ \beta & \text{if } Q_{k,t-1}=0 \text{ and } F_{k,t-1}=1 \end{cases} \tag{3}$$

On the other hand, the temporal evolution of the fire probability is given by:

$$p(F_{k,t}=1|F_{k,t-1},Q_{k,t-1}) = \begin{cases} 0 & \text{if } Q_{k,t-1}=1, \forall F_{k,t-1} \\ 0 & \text{if } F_{k,t-1}=0 \,\forall Q_{k,t-1} \\ 1 & \text{if } Q_{k,t-1}=0 \text{ and } F_{k,t-1}=1 \end{cases} \tag{4}$$

that is, as long as there is fuel, a cell keeps burning if there was fire the previous time instant.

The spatial relation should encode the effect of fire propagation. In the simple model considered here, the fire can propagate from one cell to its neighbors and, therefore, the state of its neighbor cells $R(k)$ affects the current state of each cell k. This relation is modeled mainly by parameter ω_j (whose value can depend on wind information if available). Equation (5) defines the model.

$$p(F_{k,t}=1|Q_{k,t-1},F_{j,t-1}) = \begin{cases} 0 & \text{if } j \notin R(k) \\ \omega_j & \text{if } F_{j,t-1}=1 \text{ and } j \in R(k) \text{ and } Q_{k,t-1}=0 \\ 0 & \text{if } F_{j,t-1}=0 \text{ or } Q_{k,t-1}=1 \end{cases} \tag{5}$$

Of course, fire propagation follows more complex laws (it can be transported by wind, if there are trees then it can spread through the treetops, etc.). This model is similar to the EMBYR model [14] employed in [5]. Again, it should be stressed that the main motivation of the motion model is to take into account in the estimation process the uncertainties in the fire front position due to the motion of the fire. It is not the objective to model this propagation. Nevertheless, more complex models of fire propagation could be included within the system.

Combining the previous equations lead to the prediction lines 2 and 3 of Alg. 1:

$$\bar{f}_{k,t} = (1 - q_{k,t-1})(\underbrace{f_{k,t-1}}_{Temporal} + \underbrace{\frac{1}{|R(k)|} \sum_{j \in R(k)} \omega_j f_{j,t-1}}_{Spatial}) \tag{6}$$

$$\bar{q}_{k,t} = q_{k,t-1} + (1 - q_{k,t-1})(\beta f_{k,t-1}) \tag{7}$$

where $|R(k)|$ is the number of neighbor cells considered. That is, the fire probability at a given cell depends on the previous probability and that of the neighbor cells (if the cell is not exhausted). The value q_k is increased if there is fire in the cell.
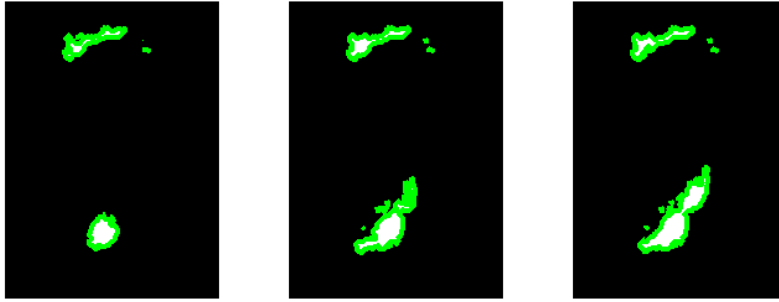
Fig. 5 The fire front shape can be obtained from the boundaries of the burnt zone. The figure shows the evolution of the burnt zone during one experiment.

3.2 Updating equations

Whenever new data are received from any vehicle of the fleet, the predicted probabilities are updated according to the Bayes rule. The important issue is to determine the likelihood functions $p(\mathbf{z}_t|F_{k,t})$ and $p(\mathbf{z}_t|Q_{k,t})$, which indicate the probability of gathering the measurements obtained given the current status of the cells. The measurements and likelihood functions will be described in the following sections of the paper.

3.3 Prior belief state and fire front shape computation

The grid is usually initiated after a fire detection mission [28], setting the Bernouilli probabilities $\{q_k\}$ to zero for all cells of the grid, and the f_k value to one for the cells corresponding to the initial estimated position of the fire. It is straightforward to include additional prior knowledge into the grid for estimation. For instance, knowledge about firewalls can be included into the q_k values of the grid, setting these values to one for places that cannot be crossed by the fire.

On the other hand, it is important to obtain the estimated position of the fire front in geolocated coordinates given the current estimated probabilities from the grid (for instance, to communicate it to the fire brigades). The fire front should be on the boundaries of the burnt zone. Also, the position of the fire front $\{\mathbf{p}_t(s)\}$ should be coherent with cells that maximize the posterior probability of fire at a given moment. Therefore, the procedure determines the boundaries of the burnt zone as the contour of regions of cells with probabilities $q_{k,t}$ over a given threshold (see Fig. 5). From these positions, the final fire front is obtained by considering connected cells on the boundary with high fire probability $f_{k,t}$.

4 Fire information extraction from on-board cameras

4.1 Fire contours extraction

The information about the fire front position is encoded in the images gathered by the UAS as the contour of fire regions on the image plane. Each vehicle in the team

processes its local images to obtain this information, which is employed to update the probabilities of the grid cells, as indicated above. The main step for obtaining the fire contours is a fire segmentation algorithm, that is applied over the images gathered by the cameras.

The infrared camera carried by the vehicles is a low-cost OEM non-thermal camera. It does not provide temperature measures but estimations of the radiation intensity throughout the scene. Thresholding is then proposed for fire segmentation. For robust fire segmentation, the thresholding technique should consider the particularities of the application. The solution adopted was to use the training-based thresholding method described in [24]. The training stage requires a set of training images and their corresponding desired threshold values given by an experienced user. The training stage identifies the conditions under which pixels should be considered to belong to the object of interest. These particularities are introduced in a system via ANFIS training method [24]. The technique used for colour images is also a training-based algorithm, similar to [33]. In the training stage, a look-up table for the RGB color space is built. The look-up table contains a Boolean value indicating whether the color represents fire or background, and is used in the application stage to classify the pixels. Both algorithms are thoroughly described in [23].

After this step, the contour of the segmented regions is obtained. However, this contour is further characterized in order to distinguish the pixels of the contour related to the fire front and the pixels related to the top of the flames, therefore obtaining the height of the flames in pixel coordinates. The dynamic properties of the fire base and the flames are used for this characterization. The position of the fire-base pixels on the image plane generally change more slowly than the position of the flame pixels (as the flames flicker). The application of a temporal low-pass filter over a sequence of consecutive segmented images is therefore used to filter out the flame pixels.

As a result of the feature extraction algorithms, the measurements $\mathbf{z}_{j,t}$ provided by each camera j on board the different UAVs are the $M_{j,t}$ pixels corresponding to the fire front $\mathbf{z}_{j,t} = \{\mathbf{z}_{j,t}(s), s = 1, \ldots, M_{j,t}\}$.

$$\mathbf{z}_{j,t}(s) = \begin{pmatrix} u_{j,t}(s) \\ v_{j,t}(s) \end{pmatrix} = \mathbf{m}_{j,t}(s), s = 1, \ldots, M_{j,t} \tag{8}$$

4.2 Eliminating image vibrations

Considering an UAS with hovering capabilities, unavoidable control errors, turbulence and vibrations produce changes in the camera position which leads to image motion. This motion can affect to the prevoiusly described algorithms and therefore, it is necessary to cancel it. Electro-mechanic systems can be used to cancel vibrations, but these systems are usually heavy, expensive and have a residual vibration.

Image processing procedures can be used for software-based image motion estimation and cancelation. This can be achieved if the apparent motion between consecutive images is computed. In this system, a sparse image motion field is computed by a feature matching algorithm. Then, this sparse motion field is used to estimate a model of the motion of the complete image. Finally, the model is applied to all pixels to warp the current image to a common frame, therefore eliminating the background motion between the current image and the previous one.
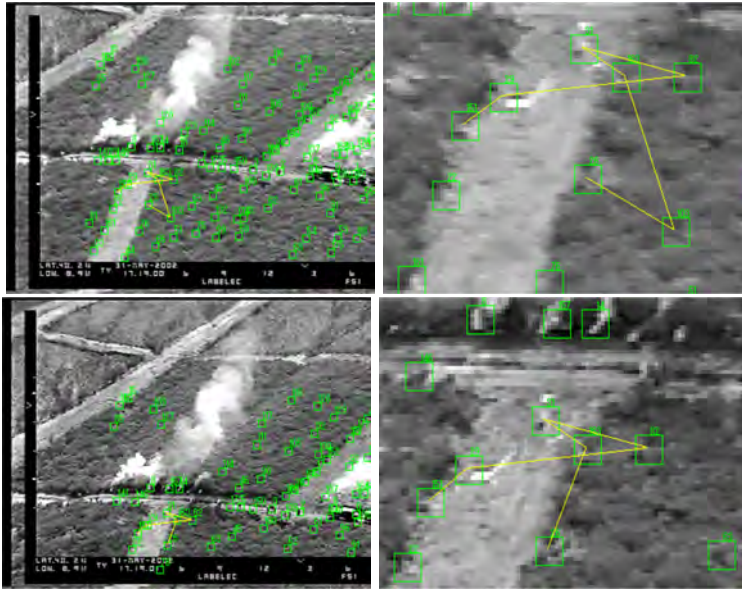
Fig. 6 Left: Interest points extracted and tracked in two consecutive images to obtain a sparse image motion field. Right: Clusters of points are used as persistent features, which allows a certain degree of invariance under rotations.

4.2.1 Description of the feature matching algorithm

The sparse motion field is computed by obtaining matches between persistent features on the image plane. Here, the method presented by Ferruz and Ollero [10] is used. The features selected are small image patches around interest points (Fig. 6, top). These features are then tracked along the sequence of images, using as a similarity measure such as the Sum of Squared Differences or Normalized Correlation over the pixels values of the image patch. Moreover, clusters of points are also used as persistent features to be tracked (Fig. 6, bottom). In this way, the features present invariant properties under certain transformations, improving the robustness of the matching between them [27].

As a result of the matching procedure, for any given pair of images, a set of matches $\{\mathbf{m}_{t-1}^{[k]}, \mathbf{m}_t^{[k]}\}$, $k = 1, \ldots, N$ is obtained.

4.2.2 Image motion model

Assuming that an UAS with hovering capabilities is used, the camera vibrations can be assimilated as small pure rotations. Considering a coordinate frame centered on the camera position at time $t-1$, following the pin-hole model [15], the homogeneous pixel coordinates $\mathbf{m}_{t-1}$ corresponding to a 3D point $\mathbf{p}$ are:

$$\eta \mathbf{m}_{t-1} = \mathbf{A} \begin{pmatrix} \mathbf{I} & \mathbf{0} \end{pmatrix} \begin{pmatrix} \mathbf{p} \\ 1 \end{pmatrix} = \mathbf{A}\mathbf{p} \tag{9}$$

with $\mathbf{A}$ the camera calibration matrix, $\mathbf{I}$ the identity and η a scale factor. If the camera only rotates, at time t the same point is imaged at pixel $\mathbf{m}_t$, with coordinates:
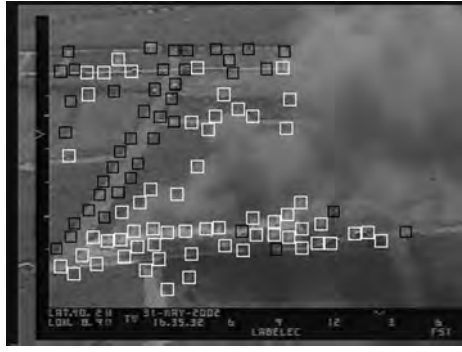
Fig. 7 Typical aerial close-range image of a fire and features selected. It can be seen how some interest points correspond to moving objects (smoke).

$$\eta' \mathbf{m}_t = \mathbf{A} \begin{pmatrix} \mathbf{R}_t & \mathbf{0} \end{pmatrix} \begin{pmatrix} \mathbf{p} \\ 1 \end{pmatrix} = \mathbf{A} \mathbf{R}_t \mathbf{p} \tag{10}$$

with $\mathbf{R}_t$ the corresponding rotation matrix. The calibration matrix $\mathbf{A}$ is invertible, so from (9) $\mathbf{p}$ can be expressed as $\mathbf{p} = \eta \mathbf{A}^{-1} \mathbf{m}_{t-1}$. Therefore,

$$\eta'' \mathbf{m}_t = \mathbf{A} \mathbf{R}_t \mathbf{A}^{-1} \mathbf{m}_{t-1} = \mathbf{H}_\infty \mathbf{m}_{t-1} \tag{11}$$

The 3×3 matrix $\mathbf{H}_\infty = \mathbf{A} \mathbf{R}_t \mathbf{A}^{-1}$ is called the *infinity homography* [15]. This homography is used as a model for the image motion under vibration. As the homography is defined up to an scale factor, it has only 8 degrees of freedom. The feature matching algorithm provide a set matches that will be used to estimate the most likely homography between two consecutive images.

4.2.3 Homography computation

From the sparse motion field given by the set of matches obtained, the objective is to infer the homographic motion model for the full image. From (11), each match $\{\mathbf{m}_{t-1}^{[k]}, \mathbf{m}_t^{[k]}\}$ adds a restriction on the homography:

$$\eta^{[k]} \mathbf{m}_t^{[k]} = \mathbf{H}_\infty \mathbf{m}_{t-1}^{[k]} \tag{12}$$

Since $\mathbf{H}$ has only eight degrees of freedom, four matches are needed to determine $\mathbf{H}_\infty$ linearly. In practice, more than four correspondences are available, and the resulting overdetermination is used to improve accuracy. A linear algorithm for the computation is provided in [15].

There are additional issues that should be considered when obtaining the model. The model derived in (11) is only valid if the points $\mathbf{p}^{[k]}$ corresponding to the matches $\{\mathbf{m}_{t-1}^{[k]}, \mathbf{m}_t^{[k]}\}$ do not move, that is, it is only valid for an static scene. However, in the case of aerial images of a forest fire, smoke and even the fire itself are moving objects that can occupy wide areas of the image (see Fig. 7). In order to compute an accurate model, these objects with *independent motion* in the scene should be detected and not considered when computing $\mathbf{H}_\infty$. These objects are treated as outliers, detected and eliminated using Least Median of Squares (LMedS) [41]. A M-Estimator is then used to obtain the final homography [30].

Fig. 8 A visual (left) and an infrared (right) images of the same fire at approximately the same time instant. Infrared images are not affected by smoke, and therefore they also provide negative information.

4.2.4 Image warping

The homography computed is used as a model for the full image motion. This model allows to relate the position of any pixel $\mathbf{m}_t$ of image I_t to its corresponding position $\hat{\mathbf{m}}_{t-1} = \mathbf{H}_\infty^{-1}\mathbf{m}_t$ in the previous image I_{t-1}. Combining consecutive transformations is possible to warp all the images to a common frame, compensating the camera motion. A method based on *pixel similarity* is employed. The method tries to minimize the RGB differences with respect to the previous image. This helps to increase the alignment between sequenced images, even correcting little errors in the homography computation. [1]

5 Fire front position updating

The fire fronts obtained with the cameras of the different UAVs are received at the ground station and used to update the probabilities of each cell of the grid. This requires the determination of the measurement models or likelihood functions $p(\mathbf{z}_t|F_{k,t})$, $p(\mathbf{z}_t|Q_{k,t})$.

Different information is carried by the fire contours in pixel coordinates, depending on its origin. As infrared images are not affected by smoke (which is transparent at these wavelengths), it is possible to employ negative information from the contours (that is, if nothing is obtained on the image plane it is very likely that there is no fire), which is not the case of visual images (see Fig. 8). The capabilities of the sensors for fire front contour detection are modeled by the values P_D (probability of detection, that is, the chance that the algorithm segment fire in the image when there is fire) and P_F (probability of false positive detection).

Furthermore, the uncertainties due to errors on the vehicle and camera pose must be accounted for as well. Each cell k has an associated 3D position $\mathbf{p}_k$ that corresponds to pixel $\mathbf{m}_{kj,t}$ on the image plane of camera of UAS j, and that can be obtained for a calibrated and localized camera using the pin-hole model:

$$\alpha \begin{pmatrix} \mathbf{m}_{kj,t} \\ 1 \end{pmatrix} = \mathbf{A}_j \left(\mathbf{R}_{j,t} \ -\mathbf{R}_{j,t}\mathbf{t}_{j,t} \right) \begin{pmatrix} \mathbf{p}_k \\ 1 \end{pmatrix} \tag{13}$$

---

[1] See the video at http://www.upo.es/isa/lmercab/video/stabiliz.mpg for a complete example on image stabilization and fire segmentation
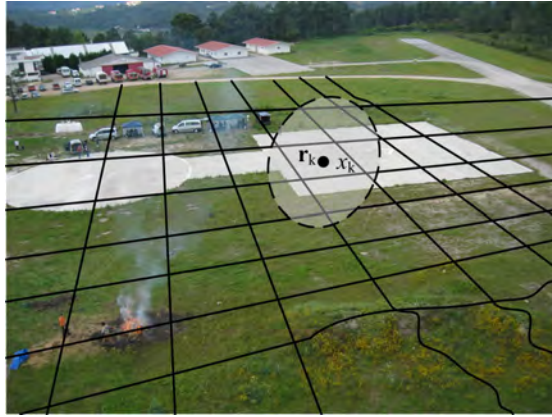
Fig. 9 The errors on the pose of the vehicles makes that each cell corresponds to an uncertainty region on the image plane.

The estimated position on the image plane of point $\mathbf{p}_k$ will be affected by the errors on the rotation $\mathbf{R}_{j,t}$ and translation $\mathbf{t}_{j,t}$ of the cameras, computed by using the navigation sensors of the UAS. These errors on the estimated position $\mathbf{m}_{kj,t}$ are approximated by a Gaussian distribution of zero mean and a certain covariance matrix $\boldsymbol{\Sigma}_{kj,t}$. As the measurement function is non-linear, these errors are estimated by using the Unscented Transformation [17] from the errors on $\mathbf{R}_{j,t}$ and $\mathbf{t}_{j,t}$ (see Fig. 9). These errors define a region $\Gamma(\mathbf{m}_{kj})$ on the image plane given by the pixels within a certain Mahalanobis distance:

$$\Gamma(\mathbf{m}_{kj}) = \mathbf{m}_j \,|\, [\mathbf{m}_j - \mathbf{m}_{kj,t}]^T \boldsymbol{\Sigma}_{kj,t}^{-1}[\mathbf{m}_j - \mathbf{m}_{kj,t}] < th \tag{14}$$

If the estimated fire front contour on the image plane $\mathbf{m}_{j,t}(s)$ passes within this region, the probabilities for cell k are updated using lines 4 and 5 of Algorithm 1 and the values:

$$p(\mathbf{z}_{j,t}|F_k = 1) = \begin{cases} P_D & \text{if } \mathbf{m}_{j,t}(s) \in \Gamma(\mathbf{m}_{kj}) \text{ for some } s \\ P_F & \text{if } \mathbf{m}_{j,t}(s) \notin \Gamma(\mathbf{m}_{kj}) \text{ for any } s \end{cases} \tag{15}$$

and

$$p(\mathbf{z}_{j,t}|F_k = 0) = \begin{cases} 1 - P_D & \text{if } \mathbf{m}_{j,t}(s) \in \Gamma(\mathbf{m}_{kj}) \text{ for some } s \\ 1 - P_F & \text{if } \mathbf{m}_{j,t}(s) \notin \Gamma(\mathbf{m}_{kj}) \text{ for any } s \end{cases} \tag{16}$$

In the same way, the probability $q_{k,t}$ is decreased for the cells corresponding to the fire front.

Infrared images provide information about places where there is no fire, as they are not occluded by smoke. For the case of visual images, however, as the fire front can be occluded by the flames, no negative information is used. This is done by setting $p(\mathbf{z}_{j,t}|F_k) = 0.5$ in the previous equations, wherever a pixel is not classified as fire (for both cases, $F_k = 1$ and $F_k = 0$).

Fig. 10 Left: the three UAVs that participated in the experiments in a coordinated flight. Right: during the demonstration, small controlled fires were performed.
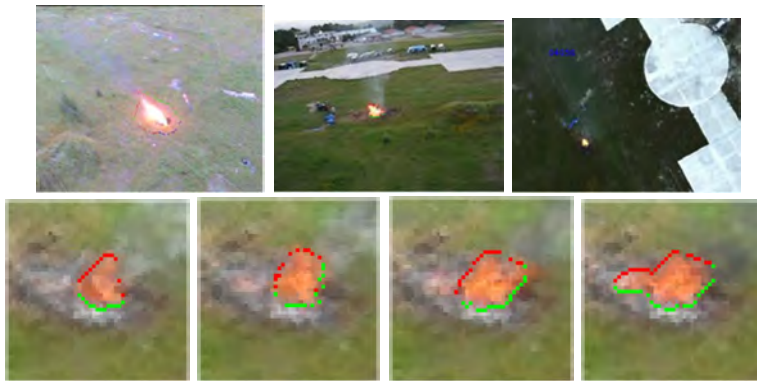

Fig. 11 Top: left, image from Heliv, after stabilization and feature extraction; middle, image from Marvin after stabilization and feature extraction; right: image from Karma. Bottom: details of the extracted contours. Green: fire front. Red: top of the flames.

6 Description of the experiments and experimental results

6.1 Fire monitoring results using an UAS with multiple vehicles

The system described in the paper was tested with a team of small-size aerial vehicles. These fire monitoring activities were included in a more general fire fighting mission, designed to demonstrate the feasibility of an UAS in this kind of scenario. In the mission, three aerial vehicles participated: the autonomous helicopter Marvin [34], Heliv [29] and the blimp Karma [16] (see Fig. 10, left).

In the general mission, summarized in [28], firstly one of the UAS (Marvin) is sent over a zone for surveillance. Marvin patrols the zone using a simple fire detector, looking for fire spots. After Marvin detects a potential fire (see Fig. 10, right), Heliv is sent to the same place for confirmation purposes (by using sensors of different modalities, see [28]) and to localize precisely the fire. After the fire is confirmed, a fire monitoring mission is generated for Marvin, Heliv and Karma, involving synchronization tasks to take and process pictures of the event from the correct viewpoints at the same time. The decisional layers of the vehicles [11] manage the task planning, allocation and the synchronization signals between UAVs in a decentralized manner, and also the

Fig. 12 An aerial view of some of the plots employed during the fire experiments at Gestosa, Portugal. The plot side in this case is around 75 m.

generation of the adequate viewpoints for monitoring the fire, covering the detected alarm from several directions (the vehicles are situated surrounding the fire with a relative orientation of 120 degrees). When the synchronization is correctly achieved, Marvin and Heliv begin to obtain pictures of the fire simultaneously and for a given time. Also, Karma is commanded to take images of all the area from a high vantage point.

The pictures from the vehicles are processed by a using the techniques described in this paper. Each UAV, locally, stabilizes the images captured by its cameras (Section 4.2) and processes the results obtaining an estimation of the position of the fire front in pixel coordinates. The data from all the systems are sent to the central station, where all the information is fused for the estimation of the evolution of the fire. Figure 11 shows the images of the same fire from the three vehicles, and how the fire contours are correctly extracted.

After the time for taking pictures has expired, Marvin and Heliv are commanded to return to home and to land. At the same time, a mapping mission is generated for Karma. Afterwards, the mission is terminated.

The full mission, involving fire detection, localization and monitoring is performed with not intervention of the operator, except for the initial plan of the mission. The experiment demonstrates the cooperation in an UAS of 3 vehicles for fire fighting, involving fire detection and monitoring[2].

6.2 Gestosa results

In the previous experiments, the controlled fires performed are of small scale, and it is difficult to appreciate an evolution on the fire front, although Fig. 11 shows how the shape of the fire is correctly estimated. The techniques described have been also validated in many controlled medium-scale forest fire experiments carried out in Serra da Gestosa (Portugal). In these field experiments, square plots of up to 150 by 100 meters were burned under controlled safety conditions. Figure 12 shows an aerial image of the Gestosa experimental site. The rectangular plots burned in the experiments

---

[2] See the video at http://www.upo.es/isa/lmercab/video/demo.mpg for a summary of the complete scenario

Fig. 13 Frames 3, 44, 77, 144 and 219 of the aerial sequence gathered during the fire experiment 520, after automatic stabilization. The extracted fire front contour is also shown.
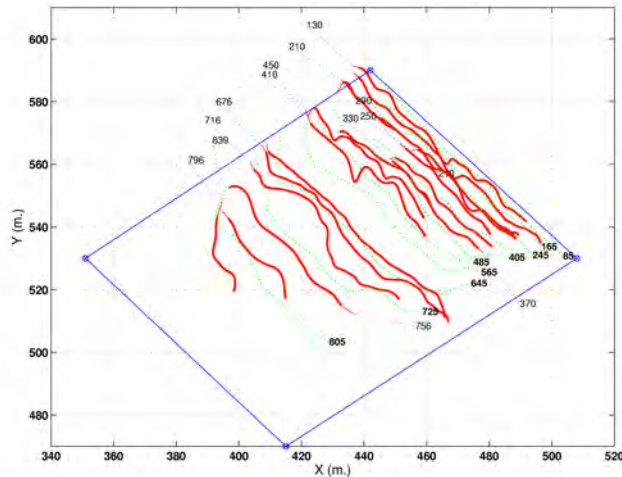

Fig. 14 Evolution of the fire front (in georeferenced coordinates) for plot 520 estimated from the images gathered by the helicopter (solid) and compared with the front obtained with an static camera (dashed).

can be observed in the images. The experiments mobilized significant resources including 80 firemen and 5 fire-fighters trucks. A more detailed description of this kind of experiments can be found in [38].

Figures 13 and 14 shows results of one of these experiments. In it, a plot of approximately 10000 square meters was burnt. In this case, a helicopter is commanded to gather aerial images.

Figure 13 shows several frames gathered from the helicopter, after the application of the image stabilization and feature extraction algorithms. It can be seen how the stabilization algorithm effectively removes the motion induced by the helicopter. It can be also seen how the fire front shape is adequately extracted from the images[3].

The fire probability grid evolves as these features are gradually considered. Figure 14 shows the estimation of the fire front shape each 20 seconds, compared to a manual estimation based also on the images (in order to validate the automatic algorithms).

These experiments show the applicability of the techniques to fires of an scale close to operational conditions.

---

[3] See the video at http://www.upo.es/isa/lmercab/video/monit.mpg for a video of the complete sequence

7 Conclusions

This paper has presented a perception system for the problem of forest fire monitoring using an UAS. The system integrates the information from the fleet of several vehicles to obtain an estimation in real time of the evolution of the forest fire. The system has been tested in actual experiments involving controlled fires. In these experiments, a fleet of three aerial systems is considered.

One of the main conclusions of the paper is that it is feasible to develop UAS for forest fire perception. The experiments show that aircraft systems can be very helpful for fire fighting activities like fire monitoring, as they can cover the gap between the spatial scales given by systems based on satellites and those based on cameras on towers. The UAS can adapt its deployment to avoid the inconveniences of other approaches, like the presence of smoke, or to cover the more convenient places.

Some issues should be discussed. One of them is the scalability of the proposed approaches. The experiments shown in the previous sections can be considered close to the operational conditions, although on a lower scale. In order to apply the techniques in real situations, vehicles with higher endurance are required. Nowadays there are vehicles, mainly developed for defense and security applications, that have the required endurance, and therefore the extension of the techniques for their use by environment management agencies seems affordable. For instance, in the FiRE project [1] a Predator is used as a platform for forest fire surveillance. Some work is also required to develop robust controllers under strong wind gusts, which are usually present in the most dangerous forest fires.

Another potential question is if the use of several UAVs offers advantages against the use of one single, very complex UAS. For the case of fire monitoring, employing several systems allows obtaining different and complementary views, and in many cases the fire is too big to be covered by just one vehicle. Moreover, small UAVs could be employed by fire brigades to, at least, obtain views of areas difficult to be accessed. Also, several cheap UAVs can carry a bench of sensors that, on the other hand, would require an usually more expensive system with a higher payload.

An additional question is whether *autonomy* is required at all for this kind of tasks. The answer is that it depends. Teleoperated vehicles can be very helpful for certain tasks, for instance for helping fire brigades to obtain close views. In any case, autonomous perception functions are required if no communication links or not enough bandwidth is available. Also, out-of-sight flights require autonomous navigation capabilities, as well as night navigation. If the UAS has to cover wide areas, then at least operational autonomy is required. The importance of higher degrees of autonomy is more evident when considering fleets with a high number of aerial vehicles. Controlling the fleet would require quite complex control centers or quite an amount of people if the vehicles are not endowed with decisional capabilities.

References

1. Ambrosia, V.: Remotely piloted vehicles as fire imaging platforms: The future is here! Wildfire Magazine (2002)
2. Ambrosia, V., Wegener, S., Sullivan, D., Buechel, S., Brass, S.D.J., Stoneburner, J., Schoenung, S.: Demonstrating UAV-Aquired Real-Time Thermal Data over Fires. Photogrametric Engineering and Remote Sensing **69**(4), 391–402 (2003)
3. Arrue, B., Ollero, A., Martínez de Dios, J.: An intelligent system for false alarm reduction in infrared forest-fire detection. IEEE Intelligent Systems **15**(3), 64–73 (2000)
4. Campbell, D., Born, W.G., Beck, J., Bereska, B., Frederick, K., Hua, S.: Airborne wildfire intelligence system: a decision support tool for wildland fire managers in Alberta. In: Proc. SPIE, Thermosense XXIV, vol. 4710, pp. 159–170 (2002)
5. Casbeer, D., Kingston, D., Bear, R., McLain, T., Li, S.: Cooperative forest fire surveillance using a team of small unmanned air vehicles. International Journal of System Science pp. 1–18 (2005)
6. Chuvieco, E., Martin, P.: A simple method for fire growth mapping using AVHRR channel 3 data. International Journal of Remote Sensing **15**, 3141–3146 (1994)
7. de Vries, J.S., Kemp, R.A.: Results with a multispectral autonomous wildfire detection system. In: Proc. SPIE Infrared Technology XX, vol. 2269, pp. 18–28 (1994)
8. Den Breejen, E., Breuers, M., Cremer, F., Kemp, R., Roos, M., Schutte, K., De Vries, J.: Autonomous forest fire detection. In: Proc. 3rd Int. Conf. on Forest Fire Research, pp. 2003–2012 (1998)
9. Dierre, D., Hoff, H., Bouchet, M.: RAPSODI: Rapid smoke detection and forest fire control. In: Int. Symposium on Forest Fire: Needs and Innovations, pp. 415–419 (1999)
10. Ferruz, J., Ollero, A.: Real-time feature matching in image sequences for non-structured environments. Applications to vehicle guidance. Journal of Intelligent and Robotic Systems **28**, 85–123 (2000)
11. Gancet, J., Hattenberger, G., Alami, R., Lacroix, S.: Task planning and control for a multi-UAV system: architecture and algorithms. In: Proc. of the IEEE/RSJ International Conference on Intelligent Robots and Systems, pp. 1017–1022 (2005)
12. Gómez Rodríguez, F., Pascual Peña, S., Arrue, B., Ollero, A.: Smoke detection using image processing. In: Proc. IV Intl. Congress on Forest Fire Research ICFFR (2002)
13. Gonzalo, J.: Fuego: A low cost service for fire detection. In: Proc. 3rd Int. Conf. on Forest Fire Research, p. 2029 (1998)
14. Hargrove, W., Gardner, R., Turner, M., Romme, W., Despain, D.: Simulating fire patterns in heterogeneous landscapes. Ecological Modelling **135**, 243–263 (2000)
15. Hartley, R., Zisserman, A.: Multiple View Geometry in Computer Vision, second edn. Cambridge University Press (2004)
16. Hygounenc, E., Jung, I.K., Soueres, P., Lacroix, S.: The Autonomous Blimp Project of LAAS-CNRS: Achievements in Flight Control and Terrain Mapping. The International Journal of Robotics Research **23**(4-5), 473–511 (2004)
17. Julier, S., Uhlmann, J.: A new extension of the kalman filter to nonlinear systems. In: Proc. of the 11th Int. Symp. on Aerospace/Defence Sensing, Simulation and Controls (1997)
18. Kelhä, V., Rauste, Y., Häme, T., Sephton, T., Buongiorno, A., Frauenberger, O., Soini, K., Venäläinen, A., San-Miguel-Ayanz, J., Vainio, T.: Combining AVHRR and ATSR satellite sensor data for operational boreal forest fire detection. International Journal of Remote Sensing **24**(8), 1691–1708 (2003)
19. Kontitsis, M., Valavanis, K., Tsourveloudis, N.: A UAV Vision System for Airborne Surveillance. In: Proc. of the IEEE International Conference on Robotics and Automation, pp. 77–83 (2004)
20. Lacroix, S., Alami, R., Lemaire, T., Hattenberger, G., Gancet, J.: Multiple Heterogeneous Unmanned Aerial Vehicles, chap. Decision Making in Multi-UAV Systems: Architecture and Algorithms. Springer Tracks on Advanced Robotics. Springer-Verlag (2007)
21. Lemaire, T., Alami, R., Lacroix, S.: A distributed tasks allocation scheme in multi-UAV context. In: Proceedings of the IEEE International Conference on Robotics and Automation, vol. 4, pp. 3622 – 3627 (2004)
22. Martínez de Dios, J., André, J., J.C.Gonçalves, Arrue, B., Ollero, A., Viegas, D.: Laboratory fire spread analysis using visual and infrared images. Intl. Journal of Wildland Fire **15**, 175–186 (2006)
23. Martínez-de Dios, J., Merino, L., Ollero, A.: Fire detection using autonomous aerial vehicles with infrared and visual cameras. In: Proc. of the 16th IFAC World Congress. Prague, Czech Republic (2005)

24. Martínez de Dios, J., Ollero, A.: A multiresolution threshold selection method based on training. Lecture Notes in Computer Science **3211**, 90–97 (2004)
25. Maza, I., Caballero, F., Capitan, J., de Dios, J.M., Ollero, A.: A distributed architecture for a robotic platform with aerial sensor transportation and self-deployment capabilities. Journal of Field Robotics **28**(3), 303–328 (2011). DOI http://dx.doi.org/10.1002/rob.20383
26. Maza, I., Caballero, F., Capitan, J., de Dios, J.M., Ollero, A.: Experimental results in multi-UAV coordination for disaster management and civil security applications. Journal of Intelligent and Robotic Systems **61**(1), 563–585 (2011). DOI 10.1007/s10846-010-9497-5
27. Merino, L., Caballero, F., Forssén, P., Wiklund, J., Ferruz, J., Martínez de Dios, J., Moe, A., Nordberg, K., Ollero, A.: Advances in Unmanned Aerial Vehicles. State of the art and the road to autonomy, chap. Single and multi-UAV relative position estimation based on natural landmarks. Springer Tracks on Advanced Robotics. Springer-Verlag (2007)
28. Merino, L., Caballero, F., Martínez de Dios, J., Ferruz, J., Ollero, A.: A cooperative perception system for multiple UAVs: Application to automatic detection of forest fires. Journal of Field Robotics **23**(3-4), 165–184 (2006)
29. Ollero, A., Alcázar, J., Cuesta, F., López-Pichaco, F., Nogales, C.: Helicopter teleoperation for aerial monitoring in the COMETS multi-UAV system. In: 3rd IARP Workshop on Service, Assistive and Personal Robots (2003)
30. Ollero, A., Ferruz, J., Caballero, F., Hurtado, S., Merino, L.: Motion compensation and object detection for autonomous helicopter visual navigation in the comets system. In: Proc. of the IEEE International Conference on Robotics and Automation, pp. 19–24 (2004)
31. Ollero, A., Lacroix, S., Merino, L., Gancet, J., Wiklund, J., Remuss, V., Veiga, I., Gutiérrez, L.G., Viegas, D.X., González, M., Mallet, A., Alami, R., Chatila, R., Hommel, G., Colmenero, F., Arrue, B., Ferruz, J., Martínez de Dios, J., Caballero, F.: Multiple eyes in the sky: Architecture and perception issues in the COMETS unmanned air vehicles project. IEEE Robotics and Automation Magazine **12**(2), 46–57 (2005)
32. Pastora, E., Águeda, A., Andrade-Cetto, J., Munoz, M., Pérez, Y., Planas, E.: Computing the rate of spread of linear flame fronts by thermal image processing. Fire Safety Journal **41**, 569–579 (2006)
33. Phillips, W., Shah, M., da Vitoria Lobo, N.: Flame recognition in video. Pattern Recogn. Lett. **23**(1-3), 319–327 (2002). DOI http://dx.doi.org/10.1016/S0167-8655(01)00135-0
34. Remuß, V., Musial, M., Hommel, G.: Marvin - an autonomous flying robot-bases on mass market. In: International Conference on Intelligent Robots and Systems, IROS. Proc. of the Workshop WS6 Aerial Robotics, pp. 23–28. IEEE/RSJ (2002)
35. San Miguel Ayanz, J., Ravail, N., Kelha, V., Ollero, A.: Active fire detection for fire emergency management: Potential and limitations for the operational use of remote sensing. Natural Hazards **35**(3), 361–376 (2005)
36. Utkin, A., Fernandes, A., oes A.V. Lavrov, F.S., Vilar, R.: Feasibility of forest-fire smoke detection using lidar. International Journal of Wildland Fire **12**(2), 159–166 (2003)
37. Viegas, D.: Forest fire propagation. Phil. Trans. R. Soc. Lond. A **356**, 2907–2928 (1998)
38. Viegas, D.X., Cruz, M., Ribeiro, L., Silva, A., Ollero, A., Arrue, B., Martínez de Dios, J., Gmez-Rodrguez, F., Merino, L., Miranda, A., Santos, P.: Gestosa fire spread experiments. In: Proc. of the IV International Congress on Forest Fire Research (ICFFR), pp. 1–13. Coimbra, Portugal (2002)
39. Viguria, A., Maza, I., Ollero, A.: SET: An algorithm for distributed multirobot task allocation with dynamic negotiation based on task subsets. In: Proceedings of the IEEE International Conference on Robotics and Automation, pp. 3339–3344. Rome, Italy (2007). DOI http://dx.doi.org/10.1109/ROBOT.2007.363988
40. Viguria, A., Maza, I., Ollero, A.: S+T: An algorithm for distributed multirobot task allocation based on services for improving robot cooperation. In: Proceedings of the IEEE International Conference on Robotics and Automation, pp. 3163–3168. Pasadena, California, USA (2008). DOI http://dx.doi.org/10.1109/ROBOT.2008.4543692
41. Zhang, Z.: Parameters estimation techniques. a tutorial with application to conic fitting. Image and Vision Computing **15**(1), 59–76 (1997)
42. Zhou, G., Li, C., Cheng, P.: Unmanned aerial vehicle (UAV) real-time video registration for forest fire monitoring. In: Proc. IEEE Intl. Geoscience and Remote Sensing Symposium IGARSS, vol. 3, pp. 25–29 (2005)